

OPEN ACCESS

Comparison of a Shastry-Sutherland lattice stability in $\text{Ce}_2\text{Pd}_2\text{Sn}$ as a function of field and doping

To cite this article: Julian G Sereni 2011 *J. Phys.: Conf. Ser.* **273** 012126

View the [article online](#) for updates and enhancements.

Related content

- [Searching for a Quantum Critical Point in Rh doped ferromagnetic \$\text{Ce}_{2-x}\text{Pd}_x\text{In}_{0.9}\$](#)
J G Sereni, M Giovannini, M Gómez Berisso et al.
- [Itinerant to local transformation and critical point in Ni-rich \$\text{Ce}_2\(\text{Ni}_y\text{Pd}_{1-y}\)_2\text{Sn}\$ alloys](#)
J G Sereni, G Schmerber, M Gómez Berisso et al.
- [Superconductivity in \$\text{Sr}\(\text{Pd}_{1-x}\text{Ni}_x\)_2\text{Ge}_2\$](#)
C D Yang, H C Hsu, W Y Tseng et al.



240th ECS Meeting ORLANDO, FL
Orange County Convention Center Oct 10-14, 2021



Abstract submission due: April 9

SUBMIT NOW

Comparison of a Shastry-Sutherland lattice stability in $\text{Ce}_2\text{Pd}_2\text{Sn}$ as a function of field and doping

Julian G. Sereni

Low Temperature Div., CAB-CNEA and CONICET, 8400 S.C. de Bariloche, Argentina

E-mail: jsereni@cab.cnea.gov.ar

Abstract. A comparative study of the stability of a Shastry-Sutherland lattice (SSL) in $\text{Ce}_2\text{Pd}_2\text{Sn}$ under different physical conditions is presented. Applied magnetic field suppresses the SSL of stoichiometric $\text{Ce}_2\text{Pd}_2\text{Sn}$ in a magnetic critical point at $T_{cr}(B) = 4.2$ K and $B_{cr} = 0.13$ T, whereas 25% of Ni does it at $T_{cr}(Ni) = 3.4$ K. Electronic concentration variation, driven by the increase of Pd (holes) concentration in $\text{Ce}_2\text{Pd}_{2+y}\text{In}_{1-y}$, decreases the magnetic transition down to $T_M = 2.8$ K in the limit of the alloy solubility, i.e. $y = 0.4$. The existence of a $M(B)$ plateau in SSL predicted by theory and the crossing of those isotherms, previously observed in the model compound $\text{SrCu}_2(\text{BO}_3)_2$ are analyzed.

1. Introduction

The Shastry-Sutherland lattice (SSL) can be described as a 2D square lattice built up from a network of dimers disposed orthogonally to each other [1]. Those dimers form from an antiferromagnetic AF coupling J between magnetic nearest-neighbors nn atoms, which interact among them through a J' coupling. Such a configuration is topologically equivalent to the 2D square lattice Heisenberg model [1] which has an exact dimer ground state. The model compound for this type of magnetic lattice is $\text{SrCu}_2(\text{BO}_3)_2$ [2], though it was recently found to form also in some intermetallic compounds with the Mo_2FeB_2 -type of structure [3].

In this contribution we present a comparative study of the SSL stability in $\text{Ce}_2\text{T}_2\text{X}$ intermetallic compounds, where T = transition metal and X = p-metal. For that purpose we have applied different control parameters, such as: i) magnetic field, ii) T = transition-metal substitution to induce a structural pressure and iii) the variation of electronic concentration (i.e. the chemical potential).

2. Experimental and results

The studied samples are polycrystalline, prepared by arc melting the appropriate amount of components. The respective annealing procedures and X-ray characterization were described elsewhere, Ref.[4] for $\text{Ce}_2\text{Pd}_2\text{Sn}$ and [5] for $\text{Ce}_2\text{Pd}_{2+y}\text{In}_{1-y}$ family. Specific heat was measured using the heat pulse technique in a semi-adiabatic He-3 calorimeter in the range between 0.5 and 20K, at zero and applied magnetic field up to 4T. DC-magnetization measurements were carried out using a standard SQUID magnetometer operating between 2 and 300K, and as a function of field up to 5T.

3. Magnetic field effect in $\text{Ce}_2\text{Pd}_2\text{Sn}$

The effect of magnetic field was investigated in stoichiometric and alloyed samples. However, for simplicity we only analyze here the results on stoichiometric $\text{Ce}_2\text{Pd}_2\text{Sn}$ which is the best example showing the main characteristics of SSL under magnetic field. In this compound, the formation of a SSL in $\text{Ce}_2\text{Pd}_2\text{Sn}$ was observed within a limited range of temperature, between an (second order) AF transition at $T_M = 4.9\text{ K}$ and a (first order) ferromagnetic FM one at $T_C = 2.1\text{ K}$ [6], having as the upper limit a correlated paramagnetic phase and a FM one at low temperature. In $\text{Ce}_2\text{Pd}_2\text{Sn}$ this exotic phase builds up from FM-dimers formed by Ce *nn* atoms, which are coupled by J . An AF J' coupling between those dimers drives the formation of the SSL, realized as a quasi 2D square lattice of effective spin $S_{eff} = 1$ below $T_M = 4.9\text{ K}$. Since the SSL only holds within a short range of temperature it is strongly affected by external magnetic field, including its suppression at a magnetic critical point: $B_{cr} = 0.13\text{ T}$ and $T_{cr} = 4.1\text{ K}$ [7].

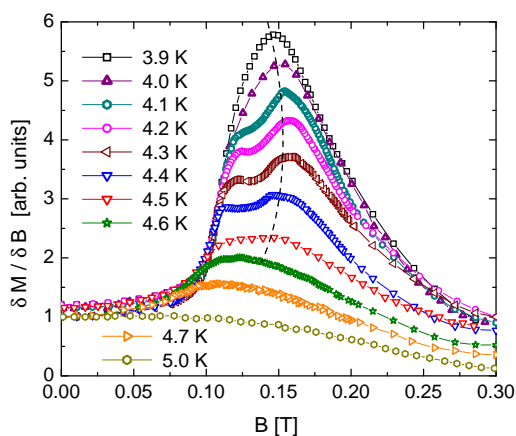


Figure 1. Detail of the $M(B)$ derivative of $\text{Ce}_2\text{Pd}_2\text{Sn}$ within the $3.9 \leq T \leq 5\text{ K}$ range showing the satellite maximum (dashed curve) around the critical field.

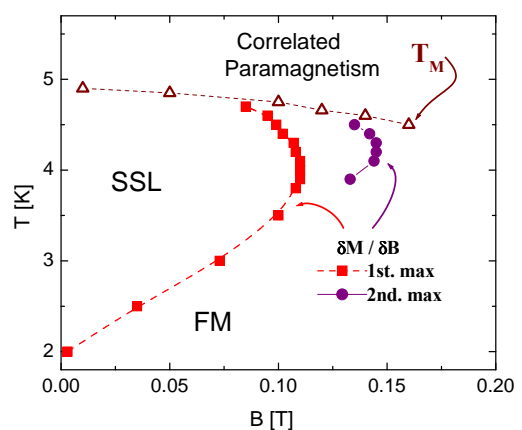


Figure 2. Phase diagram of $\text{Ce}_2\text{Pd}_2\text{Sn}$. The phase boundaries are extracted from the cusp of $M(T)$ at $T_M(B)$ \triangle , the maximum of $\partial M / \partial B$ at T \blacksquare and its satellite \bullet .

Isothermal $M(B)$ measurements show some peculiar features characteristic of the SSL, which were previously observed in the model compound $\text{SrCu}_2(\text{BO}_3)_2$ [2, 8], such as quantized magnetization plateaux at fractional values of the saturation moment M_{sat} (c.f. $1/4$ and $1/8 M_{sat}$) and the crossing of magnetization isotherms as a function of B at certain temperatures. One of those plateaux is revealed incipiently in $\text{Ce}_2\text{Pd}_2\text{Sn}$ as a satellite maximum in the $\partial M / \partial B|_T$ derivative, see Fig. 1. In the magnetic phase diagram presented in Fig. 2, the low temperature phase boundary (related to T_C) was extracted from the maximum of $\partial M / \partial B(B)|_T$ for $2 \leq T \leq 5\text{ K}$ (only shown for $T > 3.9\text{ K}$ in Fig. 2). The upper phase boundary (related to $T_M(B)$) was extracted from the cusp of $M(T)$ [7]. Around the critical region the satellite maximum of $\partial M / \partial B|_T$ indicates the field at which an incipient $M(B)$ plateau occurs, with a value $\approx 1/4 M_{sat}$. Such a plateau is related with the crossing of the $M(B)$ isotherms [7] since, within the $4 \leq T \leq 4.6\text{ K}$ range, one has $\partial M / \partial T|_{B=0} = 0$. From Maxwell relations this implies that $\partial S / \partial B|_T = 0$ and, consequently, that the entropy S is locked under field variation in an isothermal process. Therefore, a plateau is expected in those $M(B)$ isotherms. Since the existence of 'crossing points' in thermodynamical parameters carries important implications in the related properties, they were identified as 'isosbestic points' in the literature [9].

4. Structural pressure in Ni doped $\text{Ce}_2(\text{Pd}_{1-x}\text{Ni}_x)_2\text{Sn}$

The structural pressure was induced by doping the Pd lattice with smaller isoelectronic Ni atoms. In this case a weakening of the Ce magnetic moment is expected due to the Kondo screening of the $4f$ Ce states. In $\text{Ce}_2(\text{Pd}_{1-x}\text{Ni}_x)_2\text{Sn}$ that effect is observed as a reduction of the upper ordering temperature T_M as a function of Ni concentration $x(\text{Ni})$, see Fig. 3. On the contrary, the lower transition T_C to the FM phase increases with $x(\text{Ni})$ as a consequence of the reduction of the temperature range of the SSL stability. This behavior can be explained by the weakening of the J and J' couplings due to the increasing Kondo screening. Those couplings may be eventually overcome by the inter-Ce planes coupling in the 'c' crystalline direction J_C , which for $x = 0.25$ practically inhibits the formation of the SSL phase.

The arising Kondo screening is confirmed by i) the increasing γ coefficient (extracted from a $C_m/T(T \rightarrow 0)$ extrapolation), which increases proportionally to $x(\text{Ni})$ and ii) the weakening of the saturation magnetic moment at high field (not shown). In Fig. 4 we present Ni dependent phase diagram which extrapolates to a critical concentration $x_{cr}(\text{Ni}) \approx 0.27$.

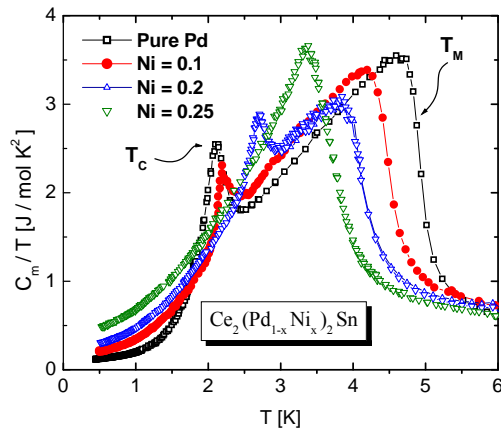


Figure 3. Thermal dependence of specific heat showing upper (T_M) and lower (T_C) transitions. The magnetic contribution C_m was evaluated after $\text{La}_2\text{Pd}_2\text{Sn}$ phonon subtraction.

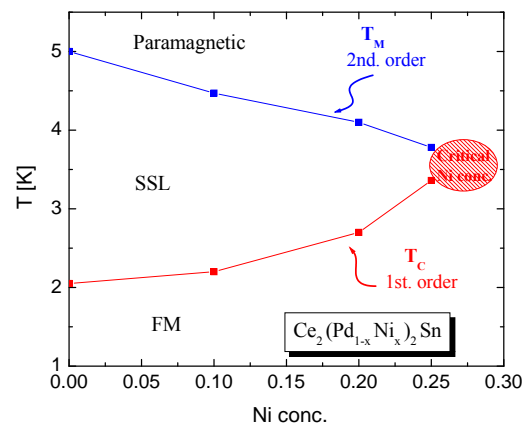


Figure 4. Ni doping dependencies of T_M and T_C , which extrapolate to a critical point at $T_{cr}(\text{Ni}) \approx 3.5$ K for $x_{cr}(\text{Ni}) \approx 0.27$, where the SSL is suppressed.

5. Electron concentration effect in $\text{Ce}_2\text{Pd}_{2+y}\text{In}_{1-y}$

The change of electronic concentration and consequently the chemical potential, is realized in the isotypic compound $\text{Ce}_2\text{Pd}_{2+y}\text{In}_{1-y}$. In that compound one takes profit of its extended range of solubility, between $0.1 \leq y \leq 0.4$ [5], where the actual Ce atomic concentration is 1.95 instead of 2. The electronic variation is induced by enriching the Pd (holes) concentration and by the replacement of $\text{Sn}[5s^25p^2]$ by $\text{In}[5s^25p^1]$.

In Fig. 5 we present the magnetic contribution to the specific heat which shows that the transition T_M decreases upon increasing $y(\text{Pd})$. In these system no T_C transition is observed but a kink (at $T = T^*$) in the $y(\text{Pd}) = 2.20$ and 0.25 alloys, which transforms into a shoulder for higher Pd concentrations. Coincidentally, only the former alloys show the SSL signs, i.e. the crossing of their $M(B)$ isotherms and a satellite maximum in $\partial S/\partial B|_{T=0}$ like in $\text{Ce}_2\text{Pd}_2\text{Sn}$. Those properties vanish for $y(\text{Pd}) = 2.35$ and 0.24 concentrations indicating that the SSL is strongly affected by the Pd/In modification which also increases atomic disorder.

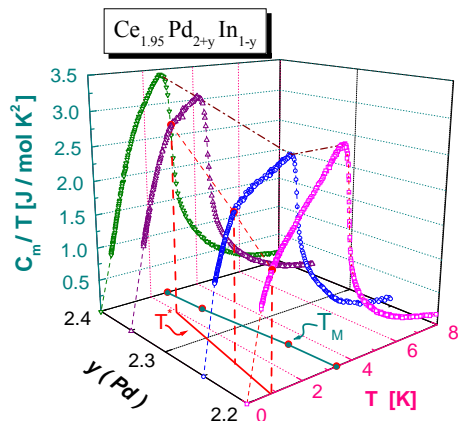


Figure 5. Magnetic specific heat dependence on temperature and $y(Pd)$ concentration. Basal plane: projection of the $y(Pd)$ dependence of T_M and T^* , see the text.

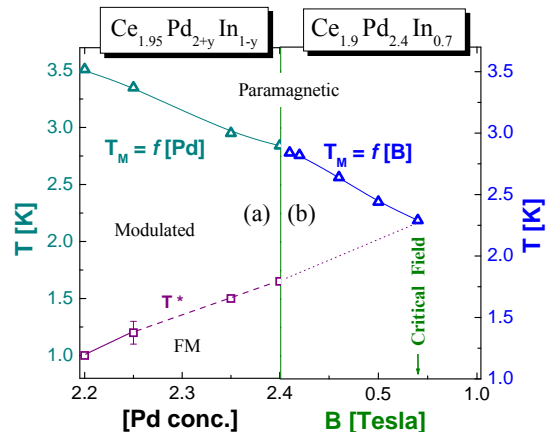


Figure 6. (a) Electronic, $y(Pd)$ holes, dependence of the T_M phase boundary and T^* . (b) Field dependence for the richest $y(Pd) = 0.24$ alloy. Dot line: extrapolation of T^* to the critical field.

Fig. 6 shows the magnetic phase diagram including both T_M and $T^*(Pd)$ dependencies. In $Ce_{1.9}Pd_{2.4}In_{0.7}$, T_M was traced down to lower temperature by applying magnetic field up to a critical value $B_{cr}(y = 0.4) = 0.7$ T where $T_{cr}(y = 0.4) = 2.3$ K. Beyond that point, a field induced FM polarization takes over. Both, $y(Pd)$ concentration and field dependencies of T_M are compared in Fig. 6 by properly scaling both parameters, c.f. Fig. 6a and b respectively.

6. Conclusions

We have compared the stability of the SSL in the Ce_2T_2X family of compounds ($T = Pd, Ni$ and $X = Sn, In$) driving different control parameters, c.f. magnetic field, structural pressure and electron concentration. We find that the SSL is suppressed in stoichiometric Ce_2Pd_2Sn by a moderate field ($B_{cr} = 0.13$ T), by arising the Kondo screening of Ce moments with $x_{cr}(Ni) \approx 0.27$ doping, and by increasing electron (holes) concentration up to $y(Pd) = 2.25$ in $Ce_{1.95}Pd_{2+y}In_{1-y}$. Comparatively, a stronger magnetic field is required to induce FM polarization in indeede compounds than in the stannides, indicating a different relation between the on-plane J and J' coupling parameters strength respect to the inter-plane J_C one.

Acknowledgments

The author thanks G. Schmerber and M. Giovannini for providing the samples, M.G.- Berisso for collaborating with the measurements and H. von Löhneysen for motivating discussions.

References

- [1] S. Miyahara and K. Ueda 1999 *Phys. Rev. Lett.* **82** 3701.
- [2] H. Kageyama et al. 1999 *Phys. Rev. Lett.* **82** 3168.
- [3] M. N. Peron et al. 1993, *J. Alloys & Comps.* **201** 203.
- [4] A. Braghta et al. 2008 *J. Magn. Magn. Mater.* **320** 1141.
- [5] M. Giovannini et al. 2000 *Phys. Rev. B* **61** 4044.
- [6] J. G. Sereni et al. 2009 *Phys. Rev. B* **80** 024428.
- [7] J. G. Sereni et al. 2010 *Phys. Rev. B* **81** 184429.
- [8] G. A. Jorge et al., 2005 *Phys. Rev. B* **71** 092403.
- [9] D. Wollhardt 1997, *Phys. Rev. Lett.* **78** 1307.